

Nucleosynthetic Constraints on the Mass of the Heaviest Supernovae

Justin M. Brown¹ and S. E. Woosley¹

ABSTRACT

Assuming a Salpeter initial mass function and taking the solar abundances as a representative sample, we explore the sensitivity of nucleosynthesis in massive stars to the truncation of supernova explosions above a certain mass. It is assumed that stars of all masses contribute to nucleosynthesis by their pre-explosive winds, but above a certain limiting main sequence mass, the presupernova star becomes a black hole and ejects nothing more. The solar abundances from oxygen to atomic mass 90 are fit quite well assuming no cut-off at all, i.e., by assuming all stars up to $120 M_{\odot}$ make successful supernovae. Little degradation in the fit occurs if the upper limit is reduced to $25 M_{\odot}$. The limit can be further reduced, but the required event rate of supernovae in the remaining range rises rapidly to compensate for the lost nucleosynthesis of the more massive stars. The nucleosynthesis of the *s*-process declines precipitously and the production of species made in the winds, e.g., carbon, becomes unacceptably large compared with elements made in the explosion, e.g., silicon and oxygen. However, by varying uncertain physics, especially the mass loss rate for massive stars and the rate for the $^{22}\text{Ne}(\alpha, n)^{25}\text{Mg}$ reaction rate, acceptable nucleosynthesis might still be achieved with a cutoff as low as $18 M_{\odot}$. This would require a supernova frequency three times greater than the fiducial value obtained when all stars explode in order to produce the required ^{16}O . The nucleosynthesis of ^{60}Fe and ^{26}Al is also examined.

Subject headings: Nucleosynthesis, Massive Stars, Stellar Evolution, Initial Mass Function, Galactic Enrichment

1. Introduction

Just which massive stars explode as supernovae and which collapse to black holes has been a topic of great interest for a long time. In particular, stellar nucleosynthesis can be used to constrain the maximum mass of the supernova that needs to (or can) explode in order to explain the abundances of the elements seen in the Sun and elsewhere (e.g. Twarog & Wheeler 1982, 1987; Maeder

¹Department of Astronomy and Astrophysics, University of California, Santa Cruz, CA 95064; jum-brown@ucsc.edu

1992). Previous works have generally focused on the production of helium and oxygen and the ratio $\Delta Y / \Delta Z$ where Y is the helium mass fraction and Z is the heavy element fraction. Maeder (1992), for example, concludes that the observed abundances are best fit if stars of all masses contribute their pre-explosive winds, but only stars below $20 - 25 M_{\odot}$ explode as supernovae (though see Prantzos (1994) who contests this conclusion). The remainder presumably end as black holes which accrete the remaining star, including all its heavy elements.

Added interest in this issue has been generated recently by the increasingly tight observational constraints placed upon the masses of presupernova stars. Smartt (2009) finds no evidence for supernova progenitors with masses over $20 M_{\odot}$. Horiuchi et al. (2011) also finds an inconsistency with the measured rate of core collapse supernovae and the cosmic star formation rate in the sense that more stars seem to form than are observed to die as supernovae by a factor of about 2. Of course, these arguments are not yet absolute. More massive supernovae may be hidden in dust and the connection between main sequence mass and presupernova mass relies on theory. Star formation rates and supernova rates are not precisely known, but these constraints may become tighter with time and certainly suggest that not all massive stars make luminous supernovae.

On the theoretical front, it has been known for a long time that more massive stars are harder to blow up than lower mass ones (e.g. Fryer 1999; Fryer & Heger 2000). With higher mass, the entropies around the collapsing iron cores are greater, and the fall off of density with radius is consequently more gradual. During the collapse this means a greater accretion rate on the proto-neutron star that is harder to reverse. O’Connor & Ott (2011) recently quantified this effect with a “compactness” parameter (see their Fig. 9) and measured the difficulty of blowing up stars in a 1D code as a function of that parameter. Their conclusion, interestingly again was that stars heavier than $20 M_{\odot}$ were harder to explode.

These considerations motivate a revisit of the problem of stellar nucleosynthesis as a function of mass. Using a fiducial model set of solar metallicity models from Woosley & Heger (2007), the same model set used by O’Connor & Ott (2011), we study the nucleosynthesis and remnant masses resulting if the supernova explosions are truncated above a certain mass, M_{BH} . A Salpeter initial mass function is assumed (Salpeter 1955) with a slope of $\Gamma = -1.35$. We determine not only the bulk nucleosynthetic properties like oxygen and remnant mass as a function of M_{BH} , but also examine the synthesis of the s -process, the individual ratios of important intermediate mass and light elements, and the synthesis of interstellar radioactivities, ^{26}Al and ^{60}Fe .

2. Models

The yield tables of Woosley & Heger (2007) give the nucleosynthesis of all species from hydrogen through lead for supernovae resulting from non-rotating massive stars with the following initial masses: 12–33 (every integer mass), 35–60 (every five masses), 60–80 (every 10 masses), 100, and 120 solar masses. The authors calculated explosions for four sets of models parameterized by the mass cut and explosion energy. Here we use their standard set for which the explosion energy was 1.2×10^{51} erg and the mass cut was located at the “entropy jump” where $S/N_A k = 4.0$. These are their “A” models and are the same models for which Zhang et al. (2008) calculated compact remnant masses and O’Connor & Ott (2011) studied compactness. The spread of these models can be seen in Fig. 1. Nucleosynthesis ejected by the pre-explosive winds and in the explosions was archived separately but is not available in Woosley & Heger (2007) (see Figure 4 in their paper for the mass loss prescription used). The values of some key species are provided in an online supplement for this paper. Using this grid of nucleosynthetic yields, we constructed a stellar population using the high-end initial mass function described by Reid & Wilson (2006) as illustrated in Fig. 1.

$$\Phi(M)d(M) \propto M^{-2.35 \pm 0.1} d(M) \quad (1)$$

The total yields of the stellar population were calculated by integrating the yields over the mass function, as described in eq. (2), where m_i is the total production (in solar masses) of isotope i , and $E_i(M)$ and $W_i(M)$ are the total ejecta of isotope i from, respectively, the supernova explosion and the winds in solar masses from a star with initial mass M :

$$m_i = \int_{12M_{\odot}}^{M_{upper}} \Phi(M)E_i(M)dM + \int_{12M_{\odot}}^{120M_{\odot}} \Phi(M)W_i(M)dM \quad (2)$$

We calculate the yields for the stable isotopes, varying the upper mass limit to the values listed in Table 1.

Our results are expressed in terms of a simple “production factor” for each isotope defined as

$$P_i = \frac{m_i / \sum_i m_i}{S_i}, \quad (3)$$

where S_i is the mass fraction of the isotope in the Sun (Lodders 2003). The importance of the production factor lies in its relationship to the supernova rate. It can be shown that the production factor from high-mass progenitors is inversely proportional to the number of supernovae estimated by the model, assuming that the majority of the isotope’s production comes from this stellar population.

For comparison, we plot the production factors as a function of atomic mass for a population with no upper bound in Fig. 2 (see also Woosley & Heger 2007).

3. Limits on M_{BH}

The mass of the heaviest supernova that has to explode is constrained by a variety of observations. These include not only the nucleosynthetic pattern of the intermediate mass elements, but especially the light component of the s -process, the frequency of supernovae, and the masses of compact remnants. The existence of a cutoff mass also has interesting implications for $\Delta Y/\Delta Z$ and the synthesis of ^{26}Al and ^{60}Fe which we also briefly discuss.

We choose to analyze the statistics of the isotopes lighter and heavier than the iron group nuclei separately as we expect the elements heavier than atomic mass 60 to be secondary nucleosynthesis due primarily to the s -process or the reprocessing of s -process isotopes in the original star. The mean and standard deviations of the production factors of the lighter and heavier iron group nuclei are tabulated separately in Table 1.

3.1. The Production of Carbon, Oxygen, and Intermediate Mass Elements

When studying the nucleosynthesis of massive stars, theorists often normalize to the production of ^{16}O , as it is the third most abundant isotope in the universe and comes almost entirely from massive stars (Langer 1996). For reference, we’ve included the production factor of ^{16}O in Table 1 as well.

In Fig. 3 we compare the production factor of various elements to that of ^{16}O for variable M_{BH} . For present purposes, success is defined as being within a factor of two of the solar abundances. We use a number of alpha elements to probe the strength of the oxygen and silicon burning, and we use ^{14}N to measure the strength of the CNO cycle. From this, it’s clear that little is lost in terms of the production of these common isotopes if the upper mass limit is reduced from 120 to 40 M_{\odot} , which supports the preliminary limits set by Heger et al. (2003).

However, for low upper mass limits, ^{12}C is overproduced in the winds compared to ^{16}O , suggesting either that this bound cannot be much lower than 25 M_{\odot} (a production factor of two) or that there is significantly less mass loss than assumed. Carbon is mostly made in the winds of very massive stars, especially during their Wolf-Rayet stage. Oxygen, which is the major part of the metallicity is also made in winds but more in the explosions. Their ratio then is quite sensitive to the mass loss prescription used. To illustrate this, in Fig. 3, we’ve also included the ratios for a population for which we’ve halved the mass loss yields. In the figure, it’s apparent that the C/O ratio remains consistent with the solar abundances down to an upper mass limit of 20 M_{\odot} . To illustrate the change in the nucleosynthesis between the upper mass limit extrema, we present Fig. 4 as a comparison to Fig. 2. The apparent large overproduction of ^{40}K in both figures is not a problem because ^{40}K is radioactive with a half life of 1.26×10^9 years (Lide 2009). Much of it

will decay before being incorporated into the Sun.

We have checked other important intermediate mass isotope ratios in order to probe how well these stellar populations represent the solar abundances. These include $^{28}\text{Si}/^{40}\text{Ca}$, $^{40}\text{Ca}/^{24}\text{Mg}$, $^{28}\text{Si}/^{56}\text{Fe}$, and $^{40}\text{Ca}/^{56}\text{Fe}$. As can be seen in Fig. 5, these all remain acceptably close to solar ratios for the entire range of M_{BH} .

3.2. The Supernova Rate

Using the production factor of ^{16}O , we can estimate how the supernova rate depends upon M_{BH} . An accurate calculation of the rate itself would require a galactic chemical evolution model that includes gas accretion onto and outflows from the galactic disk—as described in Timmes et al. (1995)—and is beyond the scope of this paper. However, we can estimate the factor by which the supernova rate would have to increase by examining N_{SN} , the total number of massive stars required to die to produce the correct amount of ^{16}O , normalized to the total number required to produce the yields of our control population ($M_{\text{BH}} = 120 M_{\odot}$). The number of stellar deaths (and therefore, supernovae) increases slowly with the lowering of the upper mass limit until approximately $40 M_{\odot}$, below which it increases rapidly up to twice the original number at $28 M_{\odot}$ and three times the original number at $19 M_{\odot}$.

3.3. The Light s -Process

The heavier component of the s -process, those nuclei above $A \approx 90$ is thought to be produced in low mass stars (Pignatari et al. 2010). The light component of the s -process, on the other hand, is generally attributed to massive stars and occurs late during helium burning when the temperature rises sufficiently for the $^{22}\text{Ne}(\alpha, n)^{25}\text{Mg}$ reaction to occur. Owing to the temperature sensitivity of this rate, production of the s -process isotopes in the mass range $A = 60 - 90$ is a potentially powerful constraint on M_{BH} . It is important that we *overproduce* the s -process elements somewhat in this stellar mass range as many of the primary isotopes are also made in lower metallicity stars that don’t produce many s -process elements.

Use of this diagnostic is complicated by the fact that many isotopes in the mass range $A = 60 - 90$ can be produced by both the s and r -processes, and so an alternative approach is to focus on a few “ s -only” isotopes (Fig. 9)—those isotopes produced exclusively by the s -process— ^{70}Ge , ^{76}Se , ^{86}Sr , and ^{87}Sr (Kappeler et al. 1989). We exclude ^{80}Kr and ^{82}Kr from our analysis—despite both being s -only isotopes—as these isotopes are also significantly produced in low-mass asymptotic giant branch stars. We notice that the s -process is most predominant in core-collapse supernovae

from 30 to 50 M_{\odot} . With more complex models of the stellar population, a comparison of the total s -process yields to the solar abundance could prove to provide greater insight as to the upper mass bound. Here, we see that ^{86}Sr and ^{87}Sr are underproduced regardless of the upper bound, which could indicate an issue with nuclear cross sections or our stellar models. The other isotopes, ^{70}Ge and ^{76}Se appear to be produced in sufficient quantities for us to use them for this paper. The production of ^{70}Ge falls below 1/2 the solar abundance at 21 M_{\odot} , whereas the production of ^{87}Sr falls below 1/2 solar production at 23 M_{\odot} . However, if we increase the rate of $^{22}\text{Ne}(\alpha, n)$ to the maximum experimental value according to Jaeger et al. (2001), we find that a limit of 18 M_{\odot} is a reasonable value for the mass of the heaviest supernovae.

3.4. ^{60}Fe and ^{26}Al

The nuclei ^{60}Fe ($\tau_{1/2} = 2.62 \times 10^6$ y) and ^{26}Al ($\tau_{1/2} = 7.17 \times 10^5$ y) are interesting because they accumulate in the interstellar medium where the emission generated by their decays can be studied using gamma-ray telescopes. Observations by Smith (2004) give a ratio for the decay rate of ^{60}Fe to that of ^{26}Al of about 0.16 implying a ratio of ^{60}Fe to ^{26}Al mass fractions of $(60/26)(0.16) = 0.37$ (Woosley & Heger 2007). As pointed out by Prantzos (2004) and discussed in Woosley & Heger (2007), current calculations give a larger value. Our current study uses yields that already address some of the concerns discussed in Woosley & Heger (2007), including inappropriate rates for ^{26}Al destruction and use of OPAL opacities for electron scattering at high temperature. As Fig. 6 shows, our mass-averaged estimate of the production is 1.0 for $M_{\text{BH}} = 120$. This compares favorably with the value 0.95 given for these models by the authors.

The remaining difference between 1.0 and 0.37 probably chiefly reflects remaining uncertainty in the neutron capture cross sections for ^{59}Fe and ^{26}Al and especially the choice of explosion energies for low mass supernovae. Studies of the light curves of Type IIp supernovae (Kasen & Woosley 2009), suggest that many supernovae, perhaps most, have an explosion energy smaller than the fiducial 1.2×10^{51} erg assumed in many studies. Reducing the explosion energy reduces the yield of ^{60}Fe substantially. Limongi & Chieffi (2006) have also emphasized the dependence of this production ratio on mass loss, convection theory, and the initial mass function. Including the effects of rotation may also increase the ^{26}Al yield (Palacios et al. 2005), especially in very massive stars.

Our purpose here is not to completely solve the debate surrounding $^{60}\text{Fe}/^{26}\text{Al}$ but to point out that the answer depends upon M_{BH} . Measurements of gamma-ray line flux ratios may thus ultimately help constrain the masses of stars that explode. Fig. 6 shows that the ratio of $^{60}\text{Fe}/^{26}\text{Al}$ produced by supernovae declines as M_{BH} becomes smaller. Given that the production of ^{60}Fe will be even smaller in those stars we are assuming still explode if their kinetic energy is reduced, this

effect could reduce the average production of ^{60}Fe appreciably.

3.5. Helium Production and $\Delta Y/\Delta Z$

As discussed extensively in Maeder (1992), the measured derivative of the helium mass fraction with respect to metallicity can, in principle, be used to constrain M_{BH} . This is because the winds of the most massive stars are rich in helium while the heavy elements are largely confined to the cores. If the cores collapse to black holes, trapping the heavy elements, the synthesis of the winds remains and increases the overall average of $\Delta Y/\Delta Z$. Observations suggest a value $\Delta Y/\Delta Z \sim 4$.

In practice, the application of this metric is fraught with uncertainty. The yields of the massive stars are dependent upon the initial mass function and especially the very uncertain mass loss rates employed. After the helium core is uncovered by mass loss, Wolf-Rayet mass loss contributes not only helium, but an increasing amount of carbon and oxygen. The remnant masses depend upon an uncertain explosion mechanism. Does all the presupernova star fall into the hole or only part? For successful explosions, where is the mass cut? Lower mass stars also contribute appreciably to both helium and metallicity and the yields of stars of all masses are sensitive to metallicity. Even an approximate meaningful result requires integration over some uncertain model for galactic chemical evolution.

However, because this metric has been applied extensively in the literature, we give in Fig. 7 our results for the solar metallicity stars considered in this survey. Until M_{BH} is reduced below $\sim 40 M_{\odot}$ $\Delta Y/\Delta Z$ remains slightly less than unity. Even for $M_{\text{BH}} = 18 M_{\odot}$, $\Delta Y/\Delta Z$ is still only 1.929, well below the observed value.

These results are, at first glance, seemingly inconsistent with those of Timmes et al. (1995) who found $\Delta Y/\Delta Z = 4$ for $M_{\text{BH}} = 17 M_{\odot}$ for solar metallicity stars and $30 M_{\odot}$ for low metallicity stars. However, Timmes et al. used the survey of Woosley & Weaver (1995) which included only stars below $40 M_{\odot}$, while our grid extends to $120 M_{\odot}$. Furthermore, Timmes et al. assumed that any winds would be metal free and not extend into the helium core. We include initial metals in the envelope and mass loss from Wolf-Rayet stars once the core is uncovered. If we redo our calculation using the assumptions of Timmes et al., the dashed curve in Fig. 7 results. This curve crosses $\Delta Y/\Delta Z$ at $M_{\text{BH}} = 17 M_{\odot}$, in excellent agreement with Timmes et al. However, we believe that our results for solar metallicity are more realistic and that a lower value of $\Delta Y/\Delta Z$ from massive stars is appropriate.

3.6. Average Mass of Compact Remnants

We use Table 4 from Zhang et al. (2008) to get the baryonic masses of the remnants for our fiducial set of supernovae from stars of initial masses of 10 to 100 M_{\odot} . We then calculate the gravitational mass of the stellar remnants with their Equation 2. We assume that the maximum gravitational mass of a neutron star is 2.0 M_{\odot} so all remnants with a higher gravitational mass than this form black holes with a gravitational mass equal to its baryonic mass. We then construct a population of stars according to a Salpeter initial mass function and vary the heaviest supernova mass. We let any star with $M > M_{\text{BH}}$ become a black hole with mass equal to its presupernova mass. In Fig. 8, we plot various quantities (the average remnant mass, the average black hole mass, the average neutron star mass, the average iron core mass, and the maximum remnant mass) as a function of M_{BH} . For those stars more massive than the heaviest supernova, we have assumed that the presupernova star completely collapses to a black hole, so our black hole masses are larger than those of Zhang et al. (2008).

We can compare this to the observed average neutron star mass from Schwab et al. (2010). From 14 neutron stars with well-measured masses, they find an average neutron star mass of $1.325 \pm 0.056 M_{\odot}$. We find an average neutron mass closest to this at 14 M_{\odot} and are within their uncertainty up to 16 M_{\odot} . This suggests that a low value for M_{BH} is more consistent with the observed neutron star masses.

4. Conclusions

By examining a variety of nucleosynthetic diagnostics, one can constrain the mass of the maximum mass supernova that must explode and not swallow up its heavy elements in a black hole. At the outset, a number of caveats are worth stating. First, our yield set from Woosley & Heger (2007) reflects a particular choice of many uncertain parameters—the treatment of convection, mass loss, key reaction rates (like $^{12}\text{C}(\alpha, \gamma)^{16}\text{O}$), and explosion physics. We lump together both means of forming a black hole, direct and by fall back and we ignore mixing. It is quite possible, probable even, that some supernovae make black holes and yet still eject some fraction of their presupernova nucleosynthesis. Mixing during the fallback epoch can complicate the estimate of yields. This probably affects the intermediate mass elements and iron more than helium, carbon, oxygen and the *s*-process. Our models sample a single metallicity—solar. While other models of different metallicity are available, using them would require a more careful treatment of galactic chemical evolution than is presently justified, given all the other uncertainties. Metallicity will not greatly affect the supernova yield of primary elements like oxygen and the intermediate mass elements, but it does affect the mass loss. We attempted to partially compensate for that by multiplying the

integrated nucleosynthesis of the wind by a constant factor of 0.5, as shown in Fig. 3. The use of solar metallicity also overestimates somewhat the production of secondary species such as the elements with odd nuclear charge and the s -process (e.g., Timmes et al. 1995), so somewhat larger yields than solar might be required than suggested by Fig. 4. Finally, all our models ignore rotation. Not only can rotation affect the mechanism and symmetry of the explosion, but it also makes the mass of the helium and carbon-oxygen core larger for a given main sequence. So our derived mass limits may actually need to be smaller.

Given these limitations, the best we can say at the present time is what supernova mass limits might be consistent with observations. The idea of a limiting mass is itself an approximation, since the compactness of the core is not a monotonic function of main sequence mass (O’Connor & Ott 2011), especially in the interesting range 20 – 35 M_{\odot} . For still heavier stars, mass loss may shrink the helium core so much that the presupernova helium core mass of say a 100 M_{\odot} star differs little from that of a 20 M_{\odot} star. Such massive stars are rare however, and their nucleosynthesis is mostly due to their presupernova winds.

We have looked at several processes that limit M_{BH} . As M_{BH} is decreased, the necessary rate of “successful” supernovae rises. For $M_{\text{BH}} = 20$ the rate is 2.88 times greater than for $M_{\text{BH}} = 120$. Surprisingly, in reducing M_{BH} to 20 M_{\odot} , the overall nucleosynthesis of most isotopes from Ne to Ca with respect to ^{16}O is altered little and the production of some isotopes in the iron group is actually improved. The greatest apparent problem is ^{22}Ne ; however, this can be mitigated somewhat by reducing the amount of mass loss or by increasing the $^{22}\text{Ne}(\alpha, n)$ rate. Of the s -process only isotopes produced mainly in massive stars, ^{70}Ge becomes the limiting isotope for the mass of the heaviest supernova, reaching half of solar value at 23 M_{\odot} . This can be extended to 18 M_{\odot} by increasing the $^{22}\text{Ne}(\alpha, n)$ rate.

In total, we find that we can easily reduce the mass of the heaviest supernovae to 40 M_{\odot} without any significant changes. For KEPLER’s standard values of nuclear rates and mass loss, there are only moderate changes in these processes down to 25 M_{\odot} . The limits become increasingly severe for smaller masses. For $M_{\text{BH}} = 25 M_{\odot}$, the stellar winds overproduce ^{12}C with respect to ^{16}O by a factor of two, unless we reduce the mass loss in these stars by two. At $M_{\text{BH}} = 21 M_{\odot}$, the lighter elements are overproduced in these more massive stars, and the s -process produces only half the needed ^{70}Ge unless the $^{22}\text{Ne}(\alpha, n)^{25}\text{Mg}$ rate is increased. At 20 M_{\odot} , even with halved mass loss, the winds overproduce ^{12}C by a factor of two.

Acknowledgements

We are grateful to Frank Timmes for very helpful correspondence concerning the calculation of $\Delta Y/\Delta Z$. This research has been supported at UCSC by the National Science Foundation (AST 0909129) and the NASA Theory Program (NNX09AK36G). JB also received support from the University of California Regent’s Fellowship Program. This research is supported in part by the Department of Energy Office of Science Graduate Fellowship Program (DOE SCGF), made possible in part by the American Recovery and Reinvestment Act of 2009, administered by ORISE-ORAU under contract no. DE-AC05-06OR23100.

REFERENCES

- Fryer, C. L. 1999, *ApJ*, 522, 413
- Fryer, C. L., & Heger, A. 2000, *ApJ*, 541, 1033
- Heger, A., Fryer, C. L., Woosley, S. E., Langer, N., & Hartmann, D. H. 2003, *ApJ*, 591, 288
- Horiuchi, S., Beacom, J. F., Kochanek, C. S., Prieto, J. L., Stanek, K. Z., & Thompson, T. A. 2011, *ApJ*, 738, 154
- Jaeger, M., Kunz, R., Mayer, A., Hammer, J. W., Staudt, G., Kratz, K. L., & Pfeiffer, B. 2001, *Physical Review Letters*, 87, 202501
- Kappeler, F., Beer, H., & Wisshak, K. 1989, *Reports on Progress in Physics*, 52, 945
- Kasen, D., & Woosley, S. E. 2009, *ApJ*, 703, 2205
- Langer, N. 1996, in *Astronomical Society of the Pacific Conference Series*, Vol. 112, *The History of the Milky Way and Its Satellite System*, ed. A. Burkert, D. H. Hartmann, & S. A. Majewski, 169
- Lide, D. R., ed. 2009, *CRC Handbook of Chemistry and Physics* (CRC Press)
- Limongi, M., & Chieffi, A. 2006, *ApJ*, 647, 483
- Lodders, K. 2003, *ApJ*, 591, 1220
- Maeder, A. 1992, *A&A*, 264, 105
- O’Connor, E., & Ott, C. D. 2011, *ApJ*, 730, 70

- Palacios, A., Meynet, G., Vuissoz, C., Knödlseeder, J., Schaerer, D., Cerviño, M., & Mowlavi, N. 2005, *A&A*, 429, 613
- Pignatari, M., Gallino, R., Heil, M., Wiescher, M., Käppeler, F., Herwig, F., & Bisterzo, S. 2010, *ApJ*, 710, 1557
- Prantzos, N. 1994, *A&A*, 284, 477
- . 2004, *A&A*, 420, 1033
- Reid, M. A., & Wilson, C. D. 2006, *ApJ*, 650, 970
- Salpeter, E. E. 1955, *ApJ*, 121, 161
- Schwab, J., Podsiadlowski, P., & Rappaport, S. 2010, *ApJ*, 719, 722
- Smartt, S. J. 2009, *ARA&A*, 47, 63
- Smith, D. M. 2004, in *ESA Special Publication*, Vol. 552, 5th INTEGRAL Workshop on the INTEGRAL Universe, ed. V. Schoenfelder, G. Lichti, & C. Winkler, 45
- Timmes, F. X., Woosley, S. E., & Weaver, T. A. 1995, *ApJS*, 98, 617
- Twarog, B. A., & Wheeler, J. C. 1982, *ApJ*, 261, 636
- . 1987, *ApJ*, 316, 153
- Woosley, S. E., & Heger, A. 2007, *Phys. Rep.*, 442, 269
- Woosley, S. E., & Weaver, T. A. 1995, *ApJS*, 101, 181
- Zhang, W., Woosley, S. E., & Heger, A. 2008, *ApJ*, 679, 639

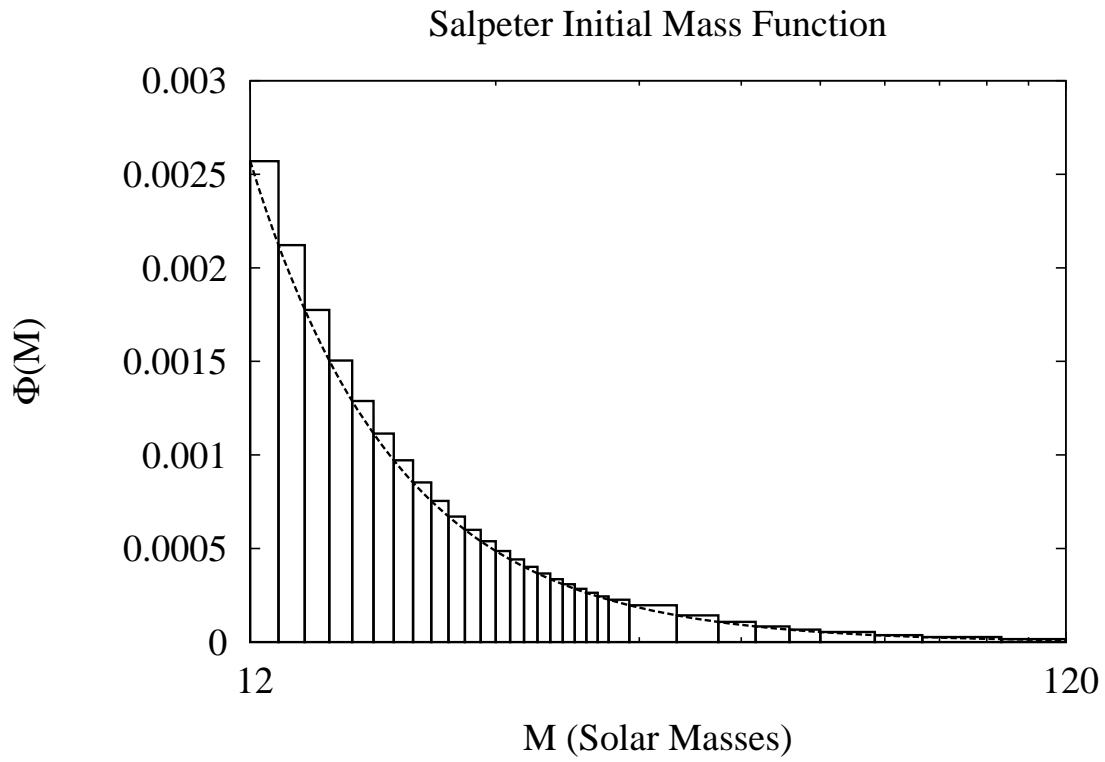


Fig. 1.— The Salpeter Initial Mass Function is a model that represents the distribution of stellar mass in a population. Mass here is plotted logarithmically. The binning indicates the binning used in our grid of stellar models.

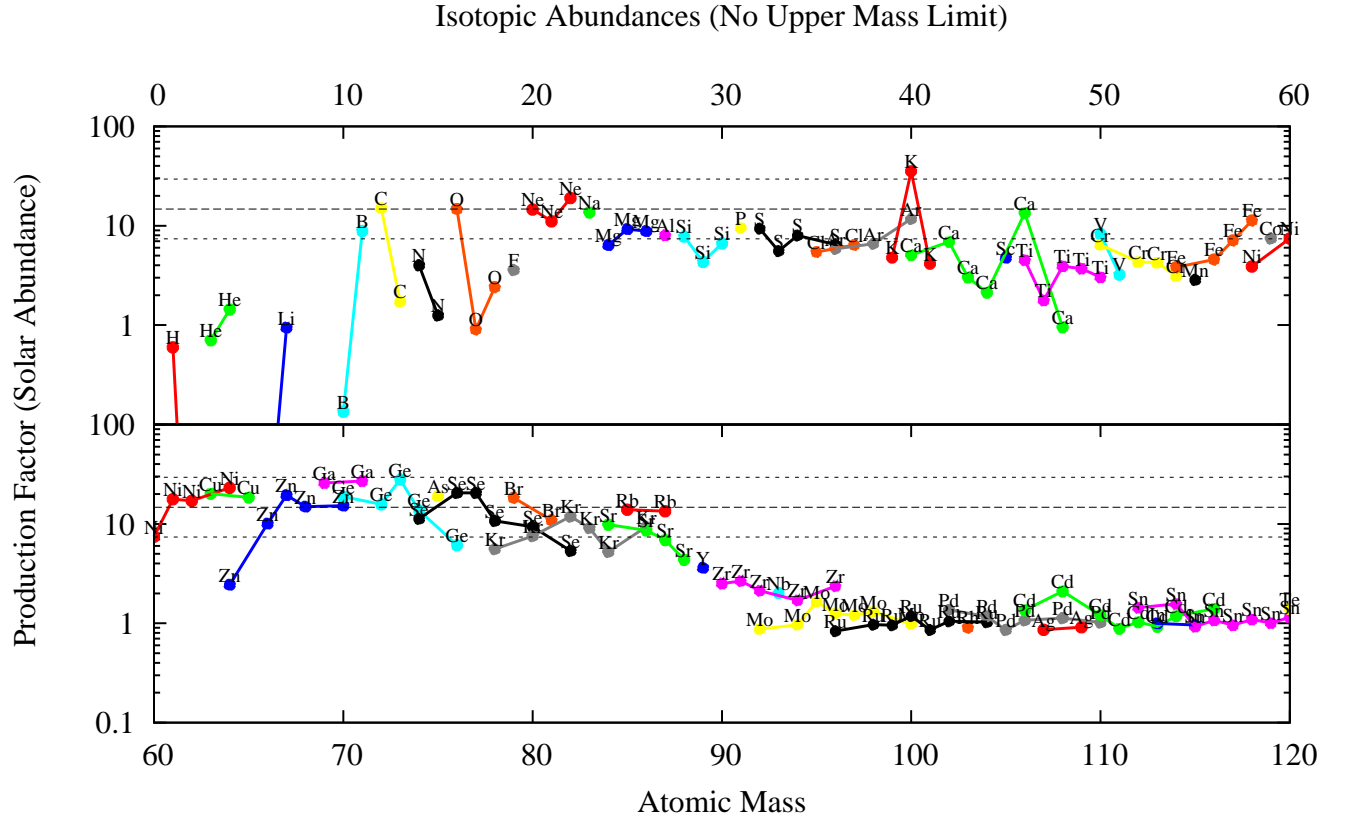


Fig. 2.— The production factor (plotted logarithmically) as a function of atomic mass. The dashed line represents the production factor of ^{16}O . The dashed lines represent a factor of two deviation from ^{16}O .

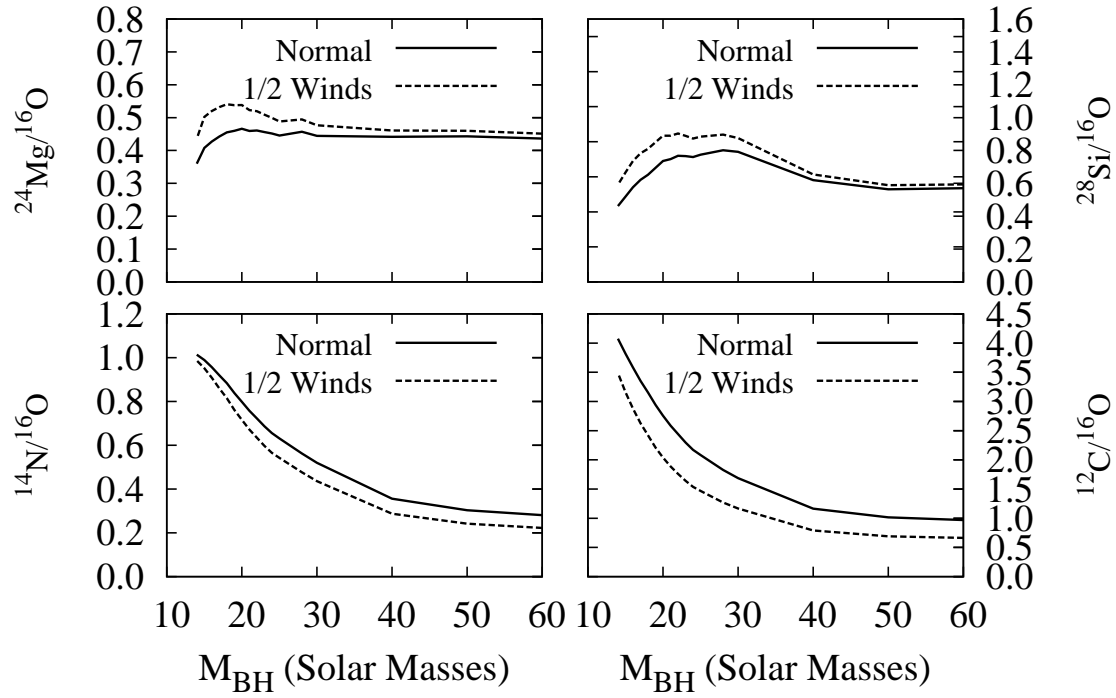


Fig. 3.— The relative abundances of the common isotopes with respect to ^{16}O as a function of M_{BH} . The plot has been truncated at $M_{\text{BH}} = 60M_{\odot}$, beyond which the abundances do not illustrate any significant variations. A relative abundance of 1 indicates solar ratio. The dotted lines represent the ratios produced if the wind contribution is halved to illustrate the dependence on wind.

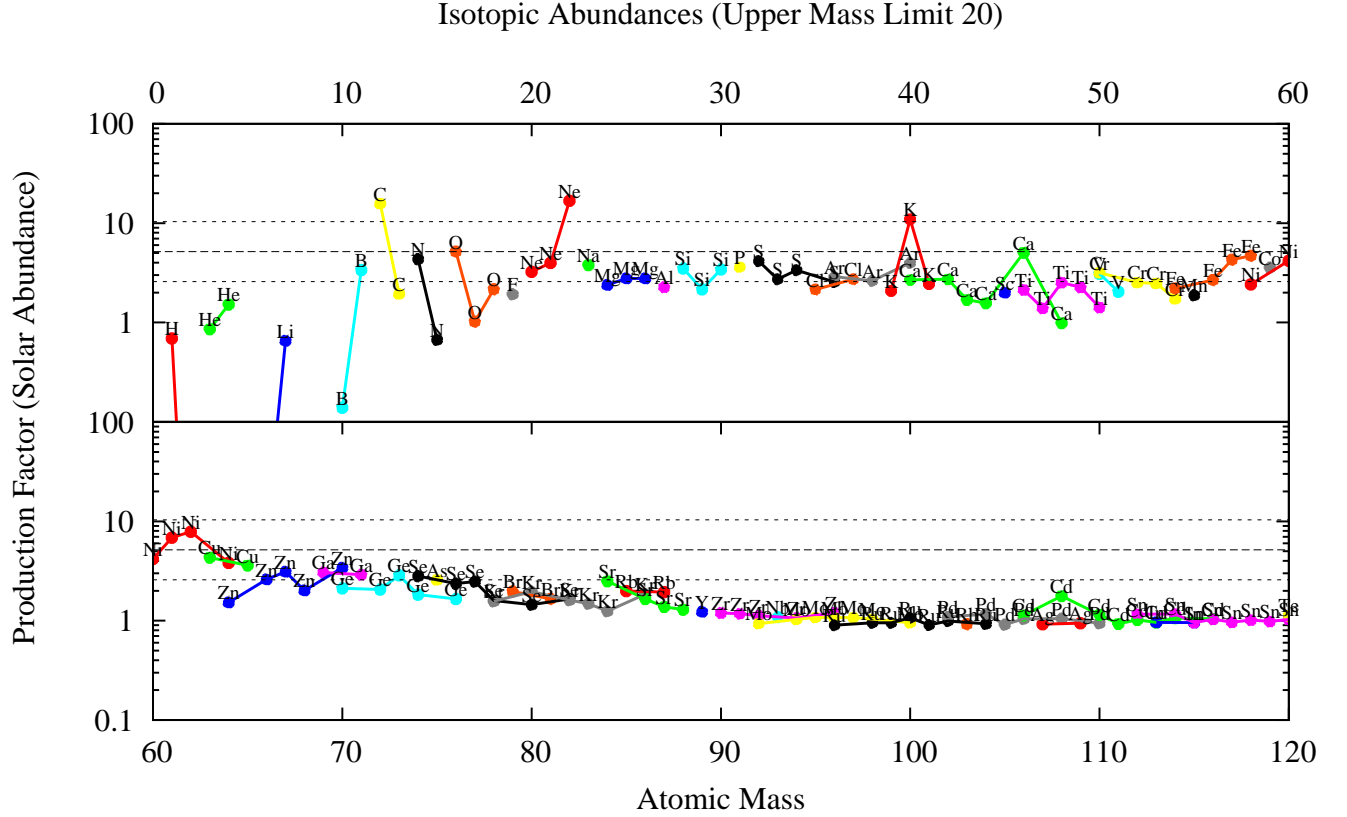


Fig. 4.— The production factor (plotted logarithmically) as a function of atomic mass. The dashed line represents the production factor of ^{16}O . The dotted lines represent a factor of two deviation from ^{16}O . Here it is assumed that all massive star over $20 M_{\odot}$ end up collapsing as black holes and their only nucleosynthetic contribution is their winds. The large abundance of ^{40}K is not a problem as this species will decay prior to solar system formation but the large abundances of ^{22}Ne and ^{12}C could indicate unresolved issues with mass loss, nuclear physics, or the assumption of a low threshold for black hole formation. The s -process is also weak here (compare with Fig. 2).

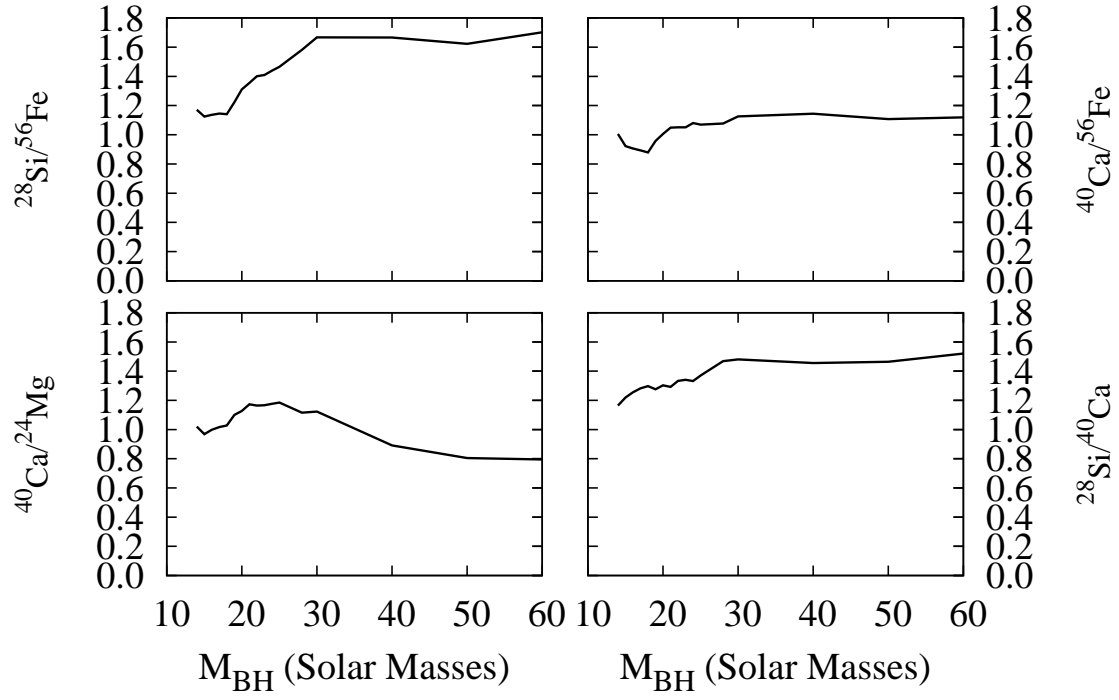


Fig. 5.— The relative abundances of the intermediate mass isotopes as a function of M_{BH} . The plot has been truncated at $M_{\text{BH}} = 60M_{\odot}$, beyond which the abundances do not illustrate any significant variations.

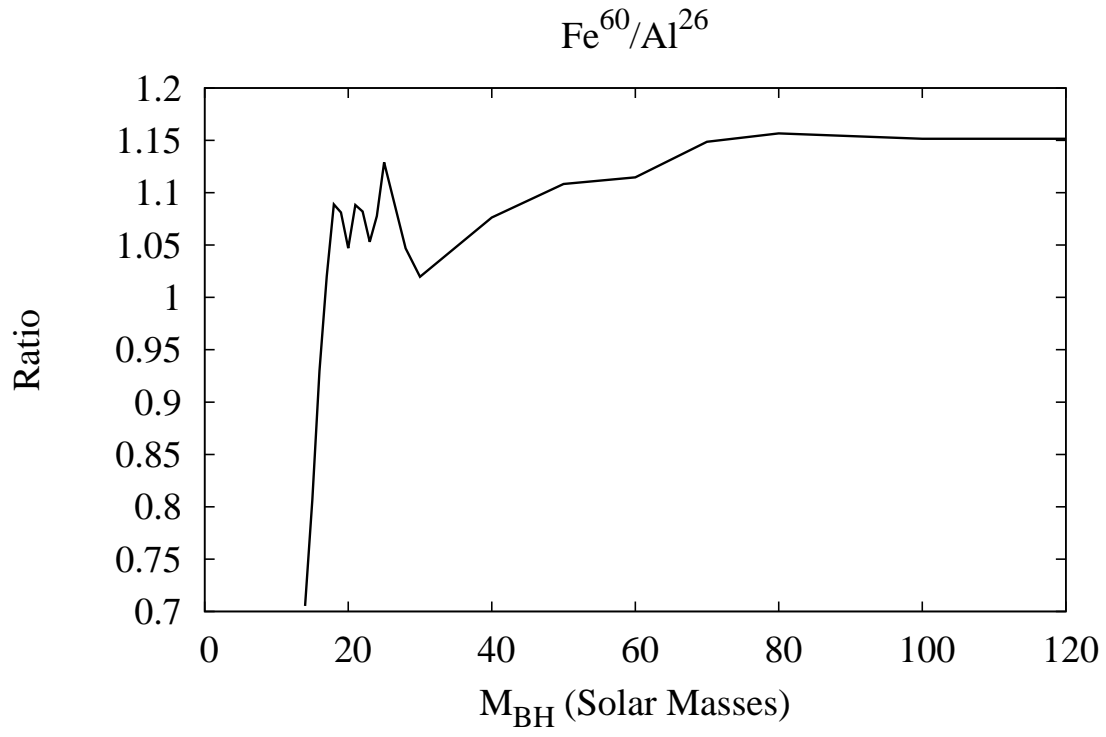


Fig. 6.— The ratio of the total masses of ^{60}Fe to ^{26}Al as a function of upper mass limit.

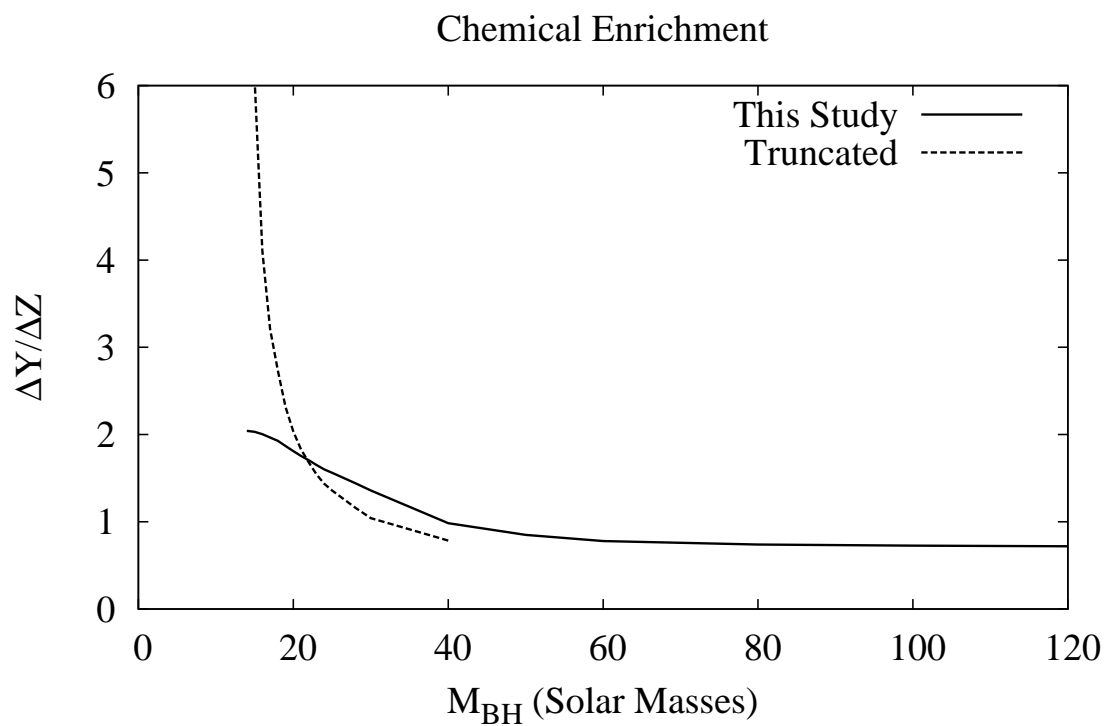


Fig. 7.— The ratio of the total deviations from the initial helium and metal mass fractions of the population as a function of the upper mass limit. The curve labeled “Truncated” uses the same assumptions as Timmes et al. (1995) in order to recreate the solar metallicity curve of Figure 37 of that same paper.

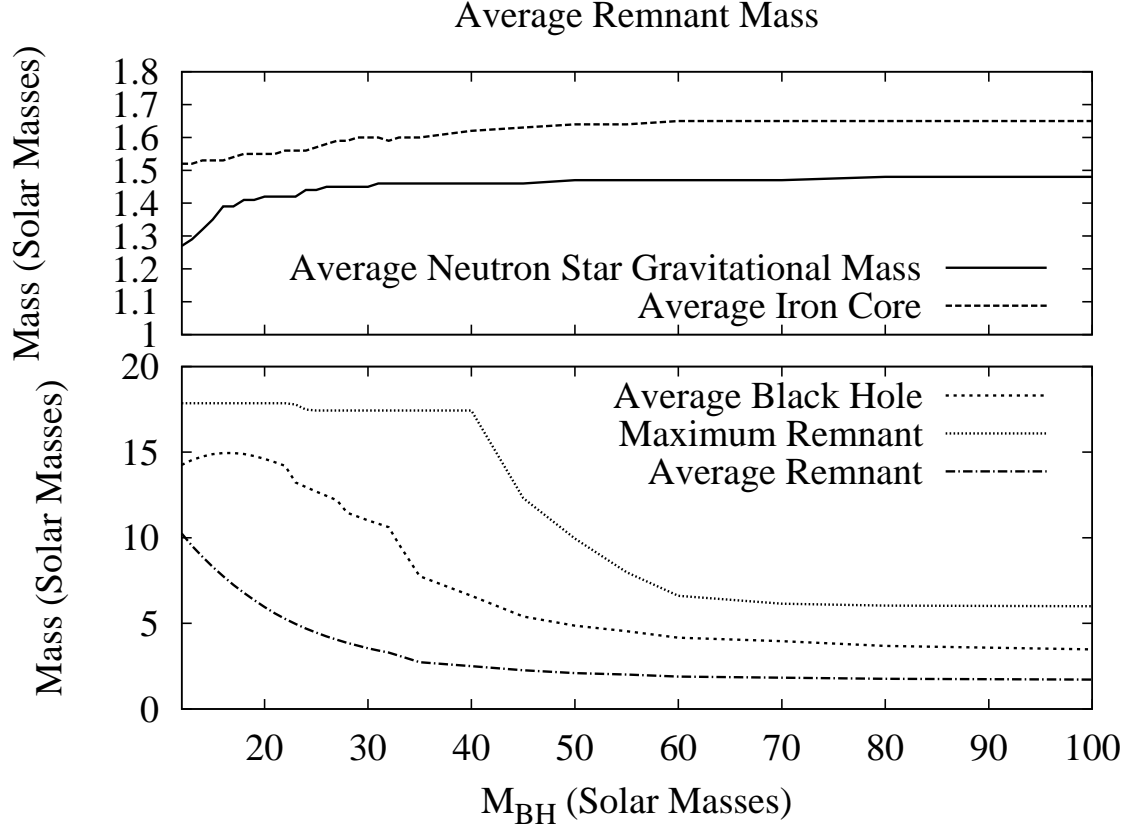


Fig. 8.— The average neutron star remnant mass, iron core mass, average black hole mass, maximum remnant mass, and average remnant mass are plotted as a function of M_{BH} . The average neutron star mass is within the observational uncertainty everywhere below $M_{\text{BH}} = 25 M_{\odot}$.

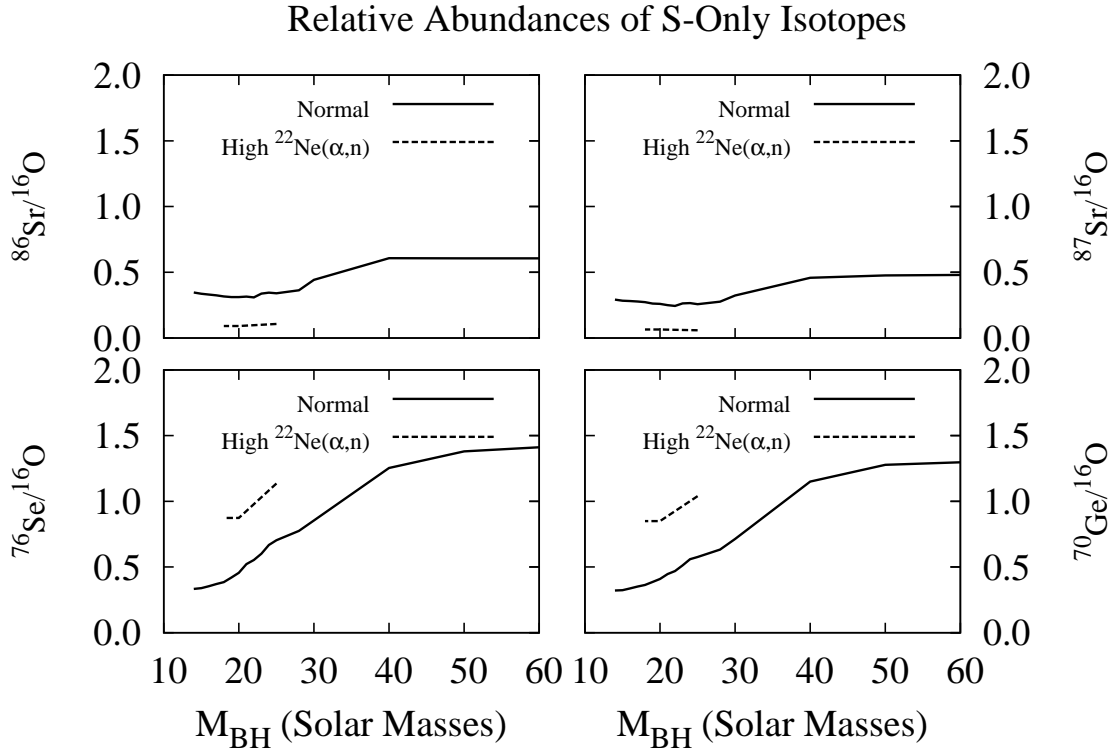


Fig. 9.— The relative abundances of the *s*-only isotopes with respect to ^{16}O and ^{24}Mg as a function of M_{upper} . The plot has been truncated at $M_{\text{upper}} = 60M_{\odot}$, beyond which the abundances do not illustrate any significant variations. A relative abundance of 1 indicates solar ratio. The dashed lines represent the ratios produced if the $^{22}\text{Ne}(\alpha, n)$ is increased to the maximum experimental value.

Table 1. Production Factor Statistics

$M_{upper} (M_{\odot})$	^{16}O	Mean (16–59)	σ (16–59)	Mean (60–84)	σ (60–84)	N_{SN}
120	14.74	6.21650	5.48443	14.59968	6.72117	1.0000000
100	14.63	6.18653	5.45782	14.54773	6.69476	1.0149254
80	14.48	6.14438	5.42532	14.48140	6.66672	1.0298507
70	14.24	6.04946	5.37006	14.34487	6.61504	1.0447761
60	14.01	5.96336	5.30620	14.16470	6.54938	1.0597014
50	13.14	5.60242	4.78830	13.20545	6.08493	1.1343282
40	11.46	5.19207	4.36852	10.63252	4.68389	1.2985075
30	7.93	4.23886	3.51987	5.86116	2.37390	1.8805970
28	7.33	3.97234	3.26334	5.26788	2.19142	2.0298507
25	6.52	3.60184	2.96335	4.35242	1.87591	2.2835820
24	6.27	3.49595	2.91884	3.95001	1.78152	2.3731341
23	5.99	3.37648	2.87740	3.59129	1.71603	2.4925373
22	5.69	3.25718	2.84823	3.29207	1.60152	2.6119401
21	5.44	3.14271	2.82677	3.01019	1.51820	2.7462685
20	5.17	3.00155	2.81088	2.69667	1.46384	2.8805971
19	4.93	2.82092	2.76516	2.51345	1.39076	3.0149255
18	4.70	2.66811	2.78619	2.30015	1.31519	3.1791043
17	4.52	2.55969	2.81806	2.11734	1.16281	3.2985075
16	4.36	2.43725	2.87535	1.94110	1.00387	3.4179103
15	4.22	2.31317	2.96168	1.78076	0.83437	3.5223880
14	4.12	2.20852	3.07487	1.60545	0.62216	3.6119401